Structural Design and Control of a Morphing Winglet to optimize the Aerodynamic Performance of the CRJ-700 Aircraft. Part 2 – Control

Paul MEYRAN[1], Hugo PAIN[1], Ruxandra Mihaela BOTEZ*,[1], Jeremy LALIBERTÉ[2]

*Corresponding author
[1]Department of Systems Engineering, École de Technologie Supérieure,
1100 Notre Dame West, Montreal, Quebec, Canada, H3C 1K3,
ruxandra.botez@etsmtl.ca
[2]Department of Mechanical and Aerospace Engineering, Carleton University,
Ottawa, Ont., Canada

DOI: 10.13111/2066-8201.2021.13.4.11

Received: 26 August 2021/ Accepted: 01 November/ Published: December 2021

Abstract: *In this study, the morphing technology was applied on winglets for the CRJ-700 transport regional aircraft with the aim to improve its aerodynamic performance. The LARCASE Virtual Research Simulator VRESIM is equipped with highest Level D certified flight data for the CRJ-700. The flight and geometrical data of the CRJ-700 were used to quantify the aerodynamic benefits of the CRJ-700 equipped with a morphing winglet versus its reference winglet. The structural design and the mechanism allowing its rotation were used to allow the orientation of the winglet with angles between 90° and -90°. The control of the orientation of the morphing winglet with its mechanism was finally carried out using the Matlab/ Simulink interface. Therefore, a new concept of morphing winglet was obtained in this research.*

Key Words: *Design, Morphing Winglet, Aerodynamics, Structure, Optimization, Control*

1. INTRODUCTION

The current aviation industry faces major environmental challenges [1]. As mentioned in Part 1 of this paper, our Laboratory of Applied Research in Aircraft Controls, Avionics and Aeroservoelasticity LARCASE team has worked already in advancing Green Aircraft Technologies in two main research axes with the aim to reduce aircraft fuel consumption. One of these axes concerns morphing aircraft and wing technologies development.

The LARCASE is equipped with four main infrastructures, that are used for research realization.

This infrastructure is composed of two Research Aircraft Flight Simulators of Level D (the highest level of certification for flight dynamics) for the Cessna Citation X business aircraft and for the CRJ-700 regional transport aircraft, the Unmanned Aerial System UAS-S4 from the Mexican company Hydra Technologies and the subsonic blow-down wind tunnel Price- Païdoussis.

The description of these equipements and of the research performed by using them is presented in [2].

On morphing wing projects, research was performed at the LARCASE in the areas of controls, structures and aerodynamics.

The major CRIAQ 7.1 project took place at the LARCASE in collaboration with Bombardier, Thales and IAR-NRC in Canada. In this project, various new methodologies were employed for the design, verification and validation of a modern controller with wind tunnel test data at the IAR-NRC on a morphing wing equipped with Smart Material Actuators and pressure sensors [3]-[5].

The major project CRIAQ MDO 505 took place also at the LARCASE in collaboration with the same partners (Bombardier, Thales and IAR-NRC in Canada) and with Italian partners from Alenia, CIRA and Federico II Naples University.

In this project, a new controller was designed, developed and validated with experimental wind tunnel test data at the IAR-NRC on a morphing wing-tip equipped with pressure sensors and electrical in-house actuators [6]-[11].

New aerodynamic methodologies were developed for morphing horizontal tail and winglet aerodynamic research on the Cessna Citation X [12]-[13], the morphing wing-tip in this CRIAQ MDO-505 project [14]-[18], as well as on the UAS-S4 and UAS-S45 several morphing wing configurations [19]-[22], including an un-swept blended winglet configuration [23].

Various morphing wing systems configurations, including a morphing camber system were designed, developed and experimentally validated in the Price-Paidoussis subsonic wind tunnel [24]-[27].

The UAS-S4 and UAS-S45 morphing wing structural analysis is presented in [28]-[29]. A new concept of morphing winglet for the CRJ-700 regional transport aircraft is proposed in this paper.

The aerodynamic performance of the CRJ-700 is optimized during the cruise flight regime by use of this morphing winglet presented, as seen in Part 1 of this paper, as well as in [30]-[31].

The structural analysis and the mechanism of the morphing winglet were developed by varying its orientation angles between 90^0 and -90^0, and they were further presented in Part 1 of this paper. In Part 2 of this paper, the control of the morphing winglet is presented.

2. MECHANISM CONTROL

The mechanisms for activating the control surfaces of an airplane wing most often use actuators.

As aviation tends to electrify these systems, today's electric actuators can handle large loads while being small, light, and reliable.

Linear electromechanical actuators used in aviation and in many fields use a DC motor, a reduction device, and a worm mechanism.

The DC motor converts electrical energy (electric current) into mechanical energy (rotational speed).

This rotational speed is adapted using a reduction box in order to control the speed of the actuator stroke.

Indeed, the screw and nut device converts a rotational movement into a translational movement.

This movement will achieve the displacement of the morphing winglet.

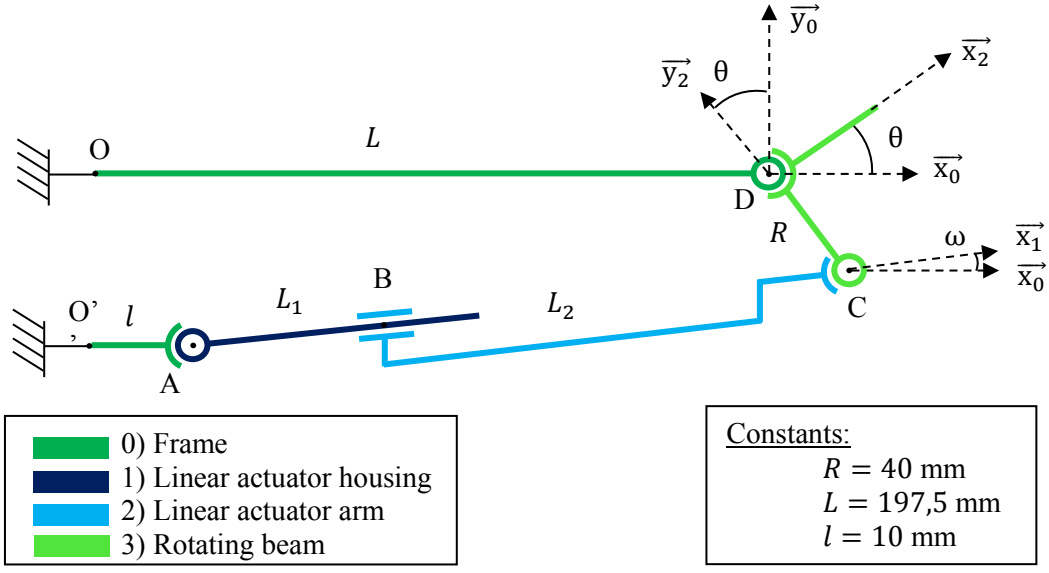

Figure 1: Kinematic diagram of the actuation system

We have defined different units of angles and length to characterize the kinematics of the actuating mechanism and in particular the angle of inclination of the winglet by the symbol θ. By performing a closed loop analysis of the mechanism, we were able to express the displacement of the actuator at point C as a function of the angle of inclination θ from its origin at point A.

$$AC(\theta) = \sqrt{[R\sin(\theta) + L - l]^2 + [R - R\cos(\theta)]^2}$$

The length of the actuator AC therefore varies according to the orientation of the morphing winglet and this parameter will allow us to characterize the position of the actuator according to its orientation. The design of a control system is based on an analysis based on a mathematical model that establishes the desired performance. Generally, the quality of the model established will demonstrate the precision associated with the model. We analyzed the system as being "linear" to simplify this part of the study. In our case, we defined the actuator as the system to be controlled. The basic model of the control system is a block diagram type diagram that will establish the structure of this control system.

We wanted to control both the orientation of the morphing winglet and the linear velocity exiting the actuator arm. Therefore, we used two controllers denoted C_1 and C_2.

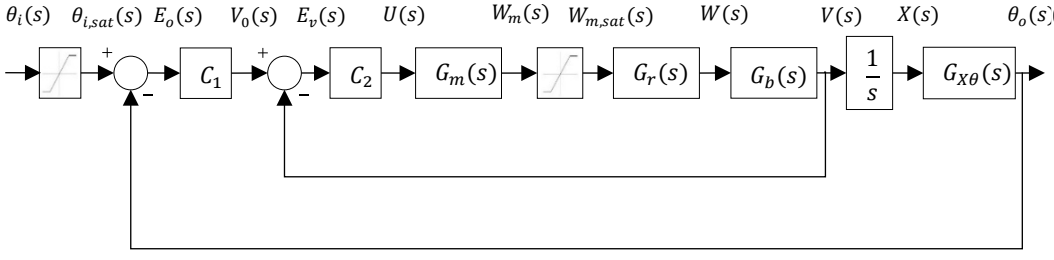

Figure 2: Block diagram of the control system

We identify the DC motor transfer function $G_m(s)$, the gear reducer transfer function $G_r(s)$, the translation arm transfer function $G_b(s)$, the integrator $\frac{1}{s}$ and the transfer function of the conversion between the actuator position and the morphing winglet orientation $G_{X\theta}(s)$.

The block associated with the motor characterizes the electromechanical behavior of the direct current motor which takes a voltage $U(s)$ as an input and provides an angular speed $W_m(s)$ as an output.

The following block produces a saturated angular velocity $W_{m,sat}(s)$ equal to $W_m(s)$ delimited by upper and lower bounds.

This step makes it possible not to exceed the limit voltage value for the correct operation of the motor and to obtain a continuous angular speed value regardless of the voltage value at the input of the motor.

The reducer located after the saturator will provide a new angular speed $W(s)$ more suited to the controlled and precise movement of the actuating arm. The latter makes it possible to convert the speed of rotation $W(s)$ into linear speed $V(s)$.

An integrator is then used to transform this linear speed $V(s)$ into a position $X(s)$ to characterize the position and movement of the actuation system. Finally, another block will convert the position of the actuator $X(s)$ into an orientation $\theta_o(s)$.

This last step therefore makes it possible to obtain the orientation of the morphing winglet from a tension.

We have integrated various blocks outside the open loop of the actuator system. First, the control system takes as input an orientation of the adaptive fin $\theta_i(s)$ which will be saturated by a saturator to ensure that the orientation is in the interval [-90 °; 90 °].

This saturated orientation $\theta_{i,sat}(s)$ is then compared with the current orientation of the output fin $\theta_o(s)$ and generates the orientation error $E_o(s)$.

The latter then constitutes the input variable of the C_1 controller which will transmit the speed $V_0(s)$ necessary to correct the orientation of the fin in its new desired orientation. This speed is then in turn compared with the actual speed of the actuator's translation arm $V(s)$ and the speed error $E_v(s)$ is then transmitted to controller C_2.

The latter will then transmit the voltage $U(s)$ necessary to the actuator to correct the speed of the translation arm of the actuation system.

After going through each of the blocks of the actuation system, we finally get the final orientation $\theta_o(s)$.

We studied the different blocks to define their associated transfer equations. To obtain the equation of the transfer function of the motor $G_m(s)$, we identified the resistance of the armature R_a, the inductance of the armature L_a, the current of the armature i_a, the input voltage of the armature U, the electromotive voltage V_b, the motor torsion T_m, the angular position of the shaft θ_m, the rotational inertia J_m, the torque constant K_t, the speed constant K_s and the viscous friction coefficient K_f.

By applying the different laws characterizing a DC motor, we have arrived at the general expression of the transfer function of the DC motor that we are going to use.

$$G_m(s) = \frac{W_m(s)}{U(s)} = \left[\frac{K_t}{(K_f + J_m s)(R_a + L_a s) + K_t K_s}\right]$$

Table 1: Motor specifications

Technical characteristics	Unit	Motor
Power P	[W]	60
Nominal voltage U_N	[V]	12
Nominal speed ω_m	[tr/min]	7 630
Nominal current i_a	[A]	4
Max efficiency η	[%]	85
Terminal resistance R_a	[Ω]	0.196
Inductivity L_a	[mH]	0.034
Torque constant K_t	[mNm/A]	13,9
Speed constant K_s	[tr/min/V]	685
Mechanical time constant K_m	[ms]	3.4
Rotor inertia J_m	[gcm^2]	33.7
Ambient temperature T_{deg}	[°C]	-30/+100

To obtain the equation of the reducer $G_r(s)$, we identified this system as a gain which will be applied to the angular speed supplied by the motor. It considers the reduction ratio r.

$$G_r(s) = \frac{1}{r}$$

To obtain the equation of the translation arm $G_b(s)$, we identified this system as being itself a gain which is applied to the angular speed of the reducer. Indeed, the linear speed is directly proportional to the rotational speed where it is necessary to consider the pitch p of the screw in the screw and nut mechanism.

$$G_b(s) = \frac{p}{2\pi}$$

Table 2: Reducer specifications

Technical characteristics	Unit	Reducer
Reduction ratio r	-	$^{421824}/_{1715}$
Max forward speed v_{max}	[mm/s]	1.1
Max advancement force F_p	[N]	1921
Efficiency η	[%]	56
Maximal pitch p_{max}	[mm]	2.13
Standardized pitch p	[mm]	2

We looked for the transfer function which considers at the input the position $X(s)$ of the actuator and at the output the winglet orientation $\theta(s)$. The actuator position was fixed at 0 mm for a 0° winglet orientation. However, the length of the AC actuator described previously in this configuration is 187.5 mm. We thus obtained a relation which defines the position according to the length of the actuator.

$$X(\theta) = AC(\theta) - 187{,}5$$

We plotted on Excel the variation of the actuator position as a function of the winglet orientation. The linear variation of this graph was finally characterized by an equation written in the form of Laplace.

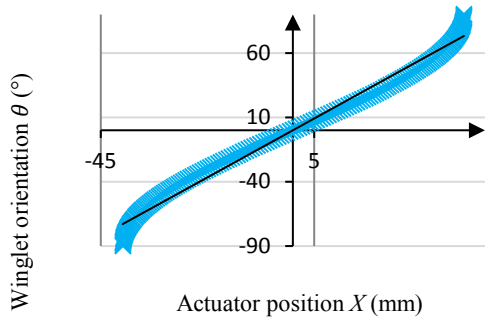

Figure 3: Variation of the morphing winglet orientation according to the position of the actuator

$$\theta(s) = 1{,}8291.X(s)$$

Ultimately, the transfer function that converts actuator position to winglet orientation simply boils down to a gain.

$$G_{X\theta}(s) = \frac{\theta(s)}{X(s)} = 1{,}8291$$

We have established the various transfer functions and we defined the suitable controller configurations for our study. We had already established that they would be PID type controllers. We carried out a study of placement of the poles and the zeros to obtain a response time and a damping which are adapted to our study. Through this study, we made sure that our system was stable by having real pole values, negative for all components. We got on the following setup using a PID for controller 1 and a PI for controller 2.

Table 3: Result of poles and zeros for morphing winglet controllers

	Controller 1	Controller 2
Type	PI	PID
Pole(s)	$-4{,}642.10^4$	$-2{,}285.10^4$ $-1{,}008.10^4$
Zeros	$-5\ 650$	$4\ 091$

$$C_1(s) = \frac{6{,}2372.10^{-41}(s + 5650)}{(s + 4{,}642.10^4)}$$

$$C_2(s) = \frac{-7{,}2252.10^{-30}(s - 4091)}{(s + 2{,}285.10^4)(s + 1{,}008.10^4)}$$

The complete morphing winglet actuation system was then modeled on Simulink. We have the entrance to the system which is modeled by a rung. The control is therefore an orientation angle of the morphing winglet. The first controller C_1 will compare the current orientation θ_s of the winglet with the command $\theta_{cmd,sat}$ and will transmit the desired linear speed for the actuator V_{cmd}. This linear speed will then be compared with the output V_s by the second controller C_2.

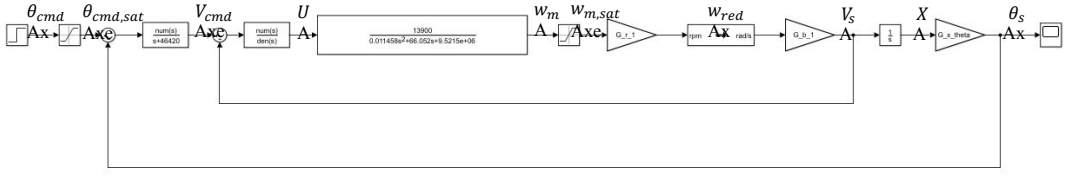

Figure 4: Simulink block diagram of the complete morphing winglet actuation system

As a result, this modeling of the morphing winglet actuation system therefore controls both the actuator speed and the orientation of the morphing winglet. We made sure that the limit conditions for morphing winglet orientations and actuator speeds were not exceeded. Also, for another motor and gearbox configuration, we would only have to change the characteristics of the controllers, but we will get much the same results. So, we got a complete control model of the morphing winglet orientation that can be considered on other similar orientation control type projects. Finally, we simulated different orientations of the morphing winglet on Simulink to make sure that all control possibilities work. We first decided to increase the orientation of the winglet gradually up to the orientation +90° through steps of 30°, then we decided to orient the winglet in a negative configuration to -45° and then to -90°. Then we made the maximum change in orientation from -90° to 90°. At the end, we reorient the winglet at 0°.

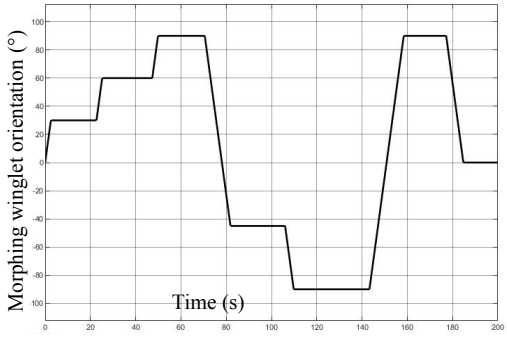

Figure 5: Evolution of the morphing winglet orientation as a function of time

6. CONCLUSIONS

A morphing winglet system was developed in Part 1 and Part 2 of this paper for the CRJ-700 regional transport aircraft for its aerodynamic performance optimization during cruise flight at the Mach number of 0.8 and altitude of 30,000 ft. In Part 1, a structure with a mechanism were developed, while in the present Part 2 of this paper, through a study of the different components of the mechanism, we obtained a control system which controls both the speed of the actuator and the inclination of the morphing winglet. From an inclination angle command, the mechanism will adapt the orientation of the morphing winglet.

ACKNOWLEDGMENTS

The research described in this paper was performed on the Virtual Research Flight Simulator for Commercial Aircraft New Technologies Development (VRESIM), which was obtained with funds from the Canada Foundation for Innovation (CFI) and Ministère de l'Économie et d'Innovation. The VRESIM was developed by Aerospace companies CAE and Bombardier for research needs of the LARCASE team.
The authors would like to thank to the Natural Sciences and Engineering Research Council of Canada NSERC for the funds received within two research programs: the CREATE Uninhabited aircraft systems Training, Innovation and Leadership Initiative (UTILI) and the Canada Research Chair Tier 1 in Aircraft Modeling and Simulation Technologies.

REFERENCES

[1] * * * ICAO. Aviation and the Environment, Montreal, Canada, 2016.

[2] R. M. Botez, Morphing Wing, UAV and Aircraft Multidisciplinary Studies at the Laboratory of Applied Research in Active Controls, Avionics and AeroServoElasticity LARCASE, *AerospaceLab Journal*, ONERA, Vol. **14**(2), pp. 1-14, https://hal.archives-ouvertes.fr/hal-01935171/, 2018.

[3] L. T. Grigorie, R. M. Botez, A. V. Popov, M. Mamou, Y. Mébarki, A Hybrid Fuzzy Logic Proportional-Integral-Derivative and Conventional On-Off Controller for Morphing Wing Actuation using Shape Memory Alloy, Part 1: Morphing System Mechanisms and Controller Architecture Design, *The Aeronautical Journal*, Vol. **116**(1179), pp. 433-449, 2012.

[4] L. T. Grigorie, R. M. Botez, A. V. Popov, M. Mamou, Y. Mébarki, A Hybrid Fuzzy Logic Proportional-Integral-Derivative and Conventional On-Off Controller for Morphing Wing Actuation using Shape Memory Alloy, Part 2: Controller Implementation and Validation, *The Aeronautical Journal*, Vol. **116**(1179), pp. 451-465, 2012.

[5] L. T. Grigorie, R. M. Botez, A.-V. Popov, How the Airfoil Shape of a Morphing Wing is Actuated and Controlled in a Smart Way, *The Journal of Aircraft Engineering*, American Society of Civil Engineers ASCE Edition, Vol. **28**(1), 2015.

[6] M. J. Tchatchueng Kammegne, L. T. Grigorie, R. M. Botez, A. Koreanschi, Design and Wind Tunnel Experimental Validation of a Controlled New Rotary Actuation System for a Morphing Wing Application, *Proceedings of the Institution of Mechanical Engineers, Part G: Journal of Aerospace Engineering*, Vol. **230**(1), pp. 132-145, 2015.

[7] M. J. Tchatchueng Kammegne, L. T. Grigorie, R. M. Botez, Design, Numerical Simulation and Experimental Testing of a Controlled Electrical Actuation System in a Real Aircraft Morphing Wing Model, *The Aeronautical Journal*, Vol. **119**(1219), pp. 1047-1072, 2015.

[8] M. J. Tchatchueng Kammegne, R. M. Botez, L. T. Grigorie, M. Mamou, Y. Mébarki, Proportional Fuzzy Feed-Forward Architecture Control Validation by Wind Tunnel Tests of a Morphing Wing, *Chinese Aeronautical Journal*, Vol. **30**(2), pp. 561-576, 2017.

[9] M. J. Tchatchueng Kammegne, Y. Tondji, R. M. Botez, L. T. Grigorie, M. Mamou, Y. Mébarki, New Control Methodology for a Morphing Wing Demonstrator, *Proceedings of the Institute of Mechanical Engineers IMechE, Part G: Journal of Aerospace*, Vol. **232**(8), pp. 1479-1494, 2017.

[10] S. Khan, T. L. Grigorie, R. M. Botez, M. Mamou, Y. Mébarki, Fuzzy Logic based Control for a Morphing Wing-Tip Actuation System: Design, Numerical Simulation and Wind Tunnel Experimental Testing, Manuscript ID: biomimetics-576000, *Biomimetics*, Vol. **4**(4), 65, Special Issue: Morphing Aircraft Systems, 2019.

[11] S. Khan, T. L. Grigorie, R. M. Botez, M. Mamou, Y. Mébarki, Novel Morphing Wing Actuator Control based Particle Swarm Optimization, *The Aeronautical Journal*, Vol. **124**(1271), pp. 55-75, 2019

[12] M. Segui, S. Bezin, R. M. Botez, Cessna Citation X Performance Improvement by an Adaptive Winglet during the Cruise Flight, *International Journal of Mechanical, Industrial and Aerospace Sciences*, vol. **11**(4), 2018.

[13] M. Segui, M. Mantilla, R. M. Botez, Design and Validation of an Aerodynamic Model of the Cessna Citation X Horizontal Stabilizer Using both OpenVSP and Digital Datcom, *International Journal of Mechanical, Industrial and Aerospace Sciences*, vol. **11**(1), 2018.

[14] A. Koreanschi, O. Sugar Gabor, J. Acotto, G. Brianchon, G. Portier, R. M. Botez, M. Mamou, Y. Mébarki, Optimization and Design of an Aircraft's Morphing Wing-Tip Demonstrator for Drag Reduction at Low Speeds, Part I - Aerodynamic Optimization using Genetic, Bee Colony and Gradient Descent Algorithms, *Chinese Journal of Aeronautics*, Vol. **30**(1), pp. 149-163, 2017.

[15] A. Koreanschi, O. Sugar Gabor, J. Acotto, G. Brianchon, G. Portier, R. M. Botez, M. Mamou, Y. Mébarki, Optimization and Design of an Aircraft's Morphing Wing-Tip Demonstrator for Drag Reduction at Low Speeds, Part II - Experimental Validation using Infra-Red Transition Measurement from Wind Tunnel Tests, *Chinese Journal of Aeronautics*, Vol. **30**(1), pp. 164-174, 2017.

[16] A. Koreanschi, O. Sugar Gabor, R. M. Botez, Drag Optimization of a Wing Equipped with a Morphing Upper Surface, *The Aeronautical Journal*, Vol. **120**(1225), pp. 473-493, 2016.

[17] A. Koreanschi, M. B. Henia, O. Guillemette, F. Michaud, Y. Tondji, O. Sugar Gabor, R. M. Botez, M. Flores Salinas, Flutter Analysis of a Morphing Wing Technology Demonstrator: Numerical Simulation and Wind Tunnel Testing, National Institute for Aerospace Research "Elie Carafoli" *INCAS Bulletin*, Vol. **8**(1), pp. 99-124, http://dx.doi.org/10.13111/2066-8201.2016.8.1.10, 2016.

[18] R. M. Botez, A. Koreanschi, O. Sugar-Gabor, I. Tondji, M. Guezguez, M. J. Tchatchueng Kammegne, L. T. Grigorie, D. Sandu, Y. Mebarki, M. Mamou, F. Amoroso, R Pecora, L. Lecce, G. Amendola, I. Dimino, A.

Concilio, Numerical and Experimental Transition Results Evaluation for a Morphing Wing and Aileron System, *The Aeronautical Journal, Smart Aircraft Issue*, Vol. **122**(1251), pp. 747-784, 2018.

[19] O. Sugar Gabor, A. Koreanschi, R. M. Botez, A New Non-Linear Vortex Lattice Method: Applications to Wing Aerodynamic Optimizations, *Chinese Aeronautical Journal*, Vol. **29**(5), pp. 1178-1195, 2016

[20] O. Sugar Gabor, A. Koreanschi, R. M. Botez, Analysis of UAS-S4 Ehécatl Aerodynamic Performance Improvement using Several Configurations of a Morphing Wing Technology, *The Aeronautical Journal*, Vol. **120**(1231), pp. 1337-1364, 2016

[21 O. Sugar Gabor, A. Simon, A. Koreanschi, R. M. Botez, Aerodynamic Performance Improvement of the UAS-S4 Ehécatl Morphing Airfoil using Novel Optimization Techniques, *Proceedings of the Institution of Mechanical Engineers, Part G: Journal of Aerospace Engineering*, Vol. **230**(7), pp. 1164-1180, 2016.

[22] O. Sugar Gabor, A. Simon, A. Koreanschi, R. M. Botez, Improving the UAS-S4 Ehecatl Airfoil High Angle of Attack Performance Characteristics using a Morphing Wing Approach, *Proceedings of the Institution of Mechanical Engineers, Part G: Journal of Aerospace Engineering*, Vol. **23**(2), pp. 118-131, 2016.

[23] H. Aubeelack, R. M. Botez, Simulation Study of the Aerodynamic Force Distributions on the UAS-S45 Baalam Wing with an Upswept Blended Winglet, *INCAS Bulletin*, Vol. **11**(1), pp. 21-38, https://doi.org/10.13111/2066-8201.2019.11.1.2, 2019.

[24] D. Communier, R. Botez, T. Wong, Design and Validation of a New Morphing Camber System by Testing in the Price–Païdoussis Subsonic Wind Tunnel, *Aerospace*, *MDPI Edition, Special Issue: Design and Analysis of Wind-Tunnel Models and Fluidic Measurements*, Vol. **7**(23), pp. 1-22, 2020.

[25] D. Communier, R. M. Botez, M. Kuitche, Experimental Validation of a New Morphing Trailing Edge System using Price-Paidoussis Wind Tunnel Tests, *Chinese Journal of Aeronautics*, Vol. **32**(6), pp. 1353-1366, 2019.

[26] A. Koreanschi, O. Sugar Gabor, R. M. Botez, Numerical and Experimental Validation of a Morphed Wing Geometry Using Price-Païdoussis Wind Tunnel Testing, *AIAA Aviation 2015*, 33rd AIAA Applied Aerodynamics Conference, Dallas, TX, USA, June 22-26, 2015.

[27] D. Communier, M. Salinas Flores, O. Carranza Moyao, R. M. Botez, Aero-Structural Modeling of a Wing using CATIA V5 and XFLR5 Software and Experimental Validation using the Price-Païdoussis Wind Tunnel, *AIAA Aviation 2015*, AIAA Atmospheric Flight Mechanics Conference, Dallas, TX, USA, June 22-26, 2015.

[28] M. Elelwi, T. Calvet, R. M. Botez, T. M. Dao, Wing Components Allocation for a Morphing Variable Span Tapered Wing using Finite Elements Method and Topology Optimization – Application to UAS-S4, *The Aeronautical Journa*l, pp. 1-24, 2021.

[29] M. Elelwi, M. A. Kuitche, R. M. Botez, T. M. Dao, Comparison and Analyses of a Variable Span Morphing of Tapered Wing with a Varying Sweep Angle, *The Aeronautical Journal*, Vol. **124**(1278), pp. 1146-1169, 2020.

[30] M. Segui, F. Abel, R. Botez & A. Ceruti, Aerodynamic Modeling of an Aircraft using Open Foam: A High Fidelity Open Source Software – Application on the CRJ-700, *The Aeronautical Journal*, 1-22, 2021

[31] M. Segui, F. R. Abel, R. M. Botez, A. Ceruti, New Aerodynamic Studies of an Adaptive Winglet Application on the Regional Jet CRJ700, *Biomimetics***,** Special Issue: Aircraft Morphing Systems 2.0, Vol. **6**(4), 54, pp. 1-28, 2021.